



## EXPERIMENTAL AND NUMERICAL INVESTIGATION OF METASTABLE FLOW OF REFRIGERANT R-22 THROUGH CAPILLARY TUBE

Esam M. Abed  
eng.isam.m@uobabylon.edu.iq  
University of Babylon, College of Engineering/ Mechanical Eng. Department.

Ammar Abdulkadhim Fathi  
eng.ammar.a.k@uobabylon.edu.iq  
University of Babylon, College of Engineering/ Mechanical Eng. Department.

### ABSTRACT

This study presents an experimental investigation of metastable region take place for refrigerant flow through adiabatic and non-adiabatic capillary tube of window type air conditioner. Large numbers of experiments are carried out to explain the effect of length of straight and helical capillary tube on metastable region under adiabatic and non-adiabatic conditions. for the case of adiabatic capillary tube, three different length are selected (70,100 and 150) cm and two helical capillary tube, the length of each tube is 100 cm with two coil diameters (2 and 6) cm. For the non-adiabatic capillary tube, the straight capillary tube suction line is 150 cm while the length of non-adiabatic helical capillary tube is 200 cm with 8 cm coil diameter. The results show that the length is the most influence parameters on beginning of metastable region. In addition the helical coil tube effect on the beginning of metastable region. As well as for the adiabatic and non-adiabatic capillary tube it is concluded that mass flow rate is the main parameters on beginning of metastable region. Also effect of length and coiling on both pressure drop and mass flow rate are discussed. The CFD commercial code, ANSYS CFX 16.1 based on finite volume method using K- $\epsilon$  turbulence model considering the homogeneous flow between phases applied to straight capillary tube. The present numerical data has been validated with the present work experimental data and with other researchers. A good agreement is obtained which can be lead to use ANSYS CFX 16.1 in the design and optimization of capillary tube in air-conditioner.

**Keywords:** metastable region, intersection point, single phase length, ANSYS CFX.

### التحقيق العملي والنظري للجريان غير المستقر لمائع التبريد R-22 خلال الانبوب الشعري

عمار عبد الكاظم فتحي

عصام مجبل عبد

#### الخلاصة

تم في هذا البحث دراسة عملية لظاهرة التغير الطوري لمائع التبريد خلال الانبوب الشعري المعزول وغير المعزول المستخدم في مكيفات الهواء. أجريت تجارب عديدة لبيان تأثير طول الانبوب الشعري على بداية التحول الطوري. حيث استخدمت الانابيب الشعرية المستقيمة الشكل وباطوال 70,100,150 سم وكذلك انابيب شعرية ملتوية بقطر لفة 6.2م لطول 100 سم. تم ربط الانبوب الشعري مع انبوب الضغط الواطئ للضاغط لكي يكون الانبوب الشعري ذو الضغط العالي على تبادل حراري انبوب الضغط الواطئ وقد درست هذا الحالة للانبوب الشعري المستقيم وبطول 150سم والانبوب الشعري الملتوي وبطول 200 سم و قطر لفة 8سم. اوضحت النتائج ان طول الانبوب الشعري هو الاكثر تأثيرا على بداية التحول الطوري. وكذلك قطر اللفة يؤثر على بداية التحول الطوري. وقد وجد ان كمية التدفق الكتلي في حالة الانبوب الشعري المعزول وغير المعزول تؤثر ايضا. تمت مناقشة طول الانبوب و قطر اللفة على انخفاض الضغط وكمية التدفق الكتلي. في الجانب النظري من هذه الدراسة تم استخدام ANSYS CFX 16.1 الميني على طريقة الحجم المحددة في محاكاة جريان مائع التبريد خلال الانبوب الشعري وباستخدام نموذج الاضطراب K- $\epsilon$  تمت مقارنة النتائج النظرية مع نتائج باحثين اخرين ومع النتائج العملية وقد وجد تطابق جيد وعليه من الممكن استخدام ANSYS CFX 16.1 في دراسة جريان مائع التبريد خلال الانبوب الشعري المستخدم في مكيفات الهواء.

**الكلمات المفتاحية:** متبدلة الاستقرار، نقطة التقاطع، طول الطور السائل ANSYS CFX.

## NOMENCLATURE

Symbol	Description	Unit
$\rho_v$	Vapor Phase Density	kg/m <sup>3</sup>
$\rho_f$	Liquid Phase Density	kg/m <sup>3</sup>
$\rho_{tp}$	Two Phase Density	kg/m <sup>3</sup>
$\mu_v$	Vapor Phase Viscosity	N.s/m <sup>2</sup>
$\mu_f$	Liquid Phase Viscosity	N.s/m <sup>2</sup>
$\mu_{tp}$	Two Phase Viscosity	N.s/m <sup>2</sup>
$S_M$	Surface Tension	N/m
$\Gamma_{fv}$	Volumetric Mass Source	Kg/m <sup>3</sup> s
$S_h$	Energy Source Term	W/m <sup>3</sup>
$\varepsilon$	Dissipation Rate Of Turbulent Kinetic Energy	m <sup>2</sup> /s <sup>3</sup>
$\mu_t$	Turbulent Viscosity	N.s/m <sup>2</sup>
$\omega$	Acentric Factor	[-]
$\sigma_k \sigma_\varepsilon C_{\varepsilon 1} C_{\varepsilon 2} C_\mu$	Constants For Standard (K. $\varepsilon$ ) Model	[-]
$k_{eff}$	Effective Thermal Conductivity	W/m.K
$C_\mu$	Correction coefficient	[-]
x	Dryness fraction	[-]
I	Single phase length	cm
II	Metastable single phase length	cm
III	Metastable two-phase length	cm
IV	Two-phase length	cm

## INTRODUCTION

Capillary tube is one of the most common devices in the air-conditioner window type which services as a pressure reduction device from condenser high pressure into evaporator lower pressure. The capillary tube is a long narrow hollow pipe with diameter range from 0.5-2 mm and length 100-600 cm [Zareh, et.al.2014]. The correct design of the capillary tubes require a full details about the metastable region which take place due to phase change from sub-cooled liquid single phase into two-phase due to frictional effect of internal wall of the capillary tube. The phase change phenomena known as flashing flow. Due to the importance of flashing flow, experimental and numerical studies are presented in the literature.

Li, et.al 1990 investigated experimentally the metastable flow phenomenon of R12 through capillary tubes with length 150 cm and diameters ranging from 0.66 – 1.17 mm.

The pressure and temperature along the capillary tube were measured precisely. The inlet temperature was varied from 290-326 °K, pressure was varied from 6.30-13.20 bar, inlet subcooling was varied from 273-290 °K. The main results are larger the diameter of the capillary tube, the lower the under pressure of vaporization and shorter the metastable length. Also it was found an increase of the inlet sub-cooling decreased the under pressure of vaporization. **Bansal and Rupasinghe 1998** presented homogeneous two-phase flow model called ,CAPIL, which was developed in order to predict the performance of adiabatic straight capillary tubes. Their mathematical model based on conservation equations of mass, momentum and energy solved numerically using finite difference method via FORTRAN. **Chen and Lin 2001** present experimental and numerical studies of R134a flow through non-adiabatic straight capillary tube of internal diameter 0.6 mm and total length is 150 cm. They obtained that metastable will appear when there is a weak heat transfer between hot capillary tube and cold suction line of compressor. **Liang and Wong 2001** simulated the refrigerant R134a flow through adiabatic straight capillary tube using equilibrium two-phase Drift flux flow model. The flow characteristics of refrigerant R134a inside capillary tube, such as distribution of pressure, dryness fraction, void fraction, phase velocities and their drift velocity relative to the center of the mass of the mixture had been presented. Their mathematical model gave information that have the ability to assist in the design of capillary tube of refrigeration systems. **Huerta, et.al. 2007** investigated experimentally the metastable flow through capillary tubes with pure propellants R134A and R600 and propellant-oil mixtures. A large number of experiments were carried out to verify the influence of inlet subcooling, internal diameter, mass flow rate and inlet pressure on the underpressure of vaporization. The results showed that the mass flow rate and subcooling degree are the two most important parameters affecting the underpressure of vaporization. Oil presence increases the metastable liquid region retarding flashing flow inception of mixture compared with pure propellant R134A.

**Imran 2008** developed a mathematical model using two-phase separated flow model to analyze the performance of capillary tubes for refrigerants R22 and R-407C through straight adiabatic capillary tubes used in an air conditioner system considering metastable region. It was found that the length of tube for R-407C is 20 % longer than that for R-22 for the same condition because the viscosity of R-407C is less than R22. **Zareh, et.al. 2014** simulated two-phase refrigerant flow using drift flux model for adiabatic straight and helically coiled capillary tubes. The model is validated with experimental results for refrigerants R134a, R12 and R22. Mass flow through the helically coiled tube with 40 mm coil diameter is compared with straight capillary tube. Reduction in the length of helically coiled capillary tubes is analyzed for the same mass flow for different coil diameters.

**Ingle, et.al. 2015** presented a homogeneous equilibrium approach to model the flashing phenomenon along with the cavitation model based on mechanism of transfer of mass through capillary tubes for systems of refrigeration. This model gave the field of pressure, temperature and dryness fraction along capillary tubes. The mass, energy and momentum of fluid equations solved using multiphase mixture model ,realizable  $k-\epsilon$  turbulent model with scalable wall function treatment had been used which is available in ANSYS FLUENT V15.0. The main conclusion is that homogeneous model can be used to design capillary tubes for refrigeration systems.

**Prajapati et al. 2016** presented numerical simulation of refrigerant flow through adiabatic capillary tube using R134a as a working fluid. ANSYS FLUENT Version 12 based on finite volume method using volume of fluid.  $k-\omega$  as a turbulent model used in CFD Simulation. A source term had been incorporated in the governing equations to model mass transfer from liquid phase to vapor phase during the flashing of liquid refrigerant. The exact location of bubble formation has been indicated.

In the present work, the metastable flow will be analyzed experimentally for refrigerant R-22 flow through straight and helical capillary tube under adiabatic and non-adiabatic conditions. Effect of various design parameters such as capillary tube length, coiling diameter and mass flow rate on the beginning of metastable region will be discussed. ANSYS CFX 16.1 based on finite volume method will be used to model the flow of refrigerant for adiabatic straight capillary tube. The proposed CFD model gives the distribution of pressure, temperature, and velocity and dryness fraction along the length of capillary tube.

## EXPERIMENTAL APPARATUS

**Figure (1a)** represents the plate of experimental rig used in the measurement of pressure and temperature of refrigerant R-22 along capillary tube. The rig contains the main components of an air conditioner window type including a rotary compressor, condenser, capillary tube and an evaporator. Schematic representation is presented in **Figure (1b)**.

Due to vaporization delay, pressure transducer (KELLER MAKE: range from 0-50 bar) had been installed along the capillary tube length and thermocouples K-type glued on the wall of the capillary tubes. As well as inlet and outlet of compressor was measured by Borden pressure gauge. Mass flow meter (Coriouis type; range 2kg/hr-500t/hr) installed in the liquid line before the test section in order to reduce the fluctuation. The present experimental work used more accurate data acquisition technique. It is known as pressure transducer technique. The pressure transducer technique is used in the present investigation to measure the pressure in all the tapes of the turbulent pipe flow of refrigerant flow through adiabatic and non-adiabatic straight and helically coiled capillary tubes with a special T-connection technique. In order to minimize the disturbance to the normal refrigerant flow, the holes with a diameter of 1 mm, were made by drilling machine in the required positions along the capillary tubes. Holes with the diameter were a little bit more than the outer diameter of the capillary which were made in copper tube with 4.68 mm diameter. Then, the capillary tube passed through pipe. One end of tubes was closed with solder and at the other end a pressure tap was installed, and connected to the pressure transducer. A detail of the T-connection design is illustrated in **Figure (2)**. The pressure transducer are connected to interface system of pressure to record the data via excel for each one second. All measuring temperatures are recorded using an interface system, named [BTM-4208SD]. The measured temperatures are showed via Microsoft Excel at each position in capillary tube for each one second. The flowmeter indicates the mass flow rate in order to study the effect of mass flow rate on the beginning of metastable region. The mass flow rate for each capillary tube is presented in **Table (1)**. The test section specification of straight and helical capillary tube under adiabatic and non-adaibatic conditions are presented in **Figure (3)**.

## NUMERICAL MODEL

On the basis of inlet boundary conditions such as inlet pressure, temperature and mass flow rate of refrigerant inside capillary tube, the flow will be turbulent. In the present numerical simulation,  $k - \varepsilon$  turbulent model will be used for better accuracy at the cost of less computational time. The creation of capillary tube model is designed by DESIGN MODELER and generation of numerical grid is presented for straight adiabatic capillary tube as in **Figure 4**.

Flashing flow of refrigerant flow through adiabatic capillary tube is simulated using commercial CFD code ANSYS CFX version 16.1 based on finite volume method using

$k - \varepsilon$  turbulence model along with Eulerian-Eulerian model considering the homogeneity between phases to solve the governing equations of continuity, energy, void fraction and momentum [ANSYS CFX 16.1]. The proposed model solves the governing equations of continuity, momentum, energy and void fraction using finite volume method. The governing equations are:

**Conservation of Mass**

$$\frac{\partial}{\partial t}(\rho_{tp}) + \nabla \cdot (\rho_{tp} U_{tp}) = 0$$

**Conservation of Momentum**

$$\frac{\partial}{\partial t}(\rho_{tp} U_{tp}) + \nabla \cdot (\rho_{tp} U_{tp} * U_{tp} - \mu(\nabla U_{tp} + (\nabla U_{tp})^T)) = S_M - \nabla p$$

**Conservation of Energy**

$$\frac{\partial}{\partial t}(\rho E) + \nabla \cdot (U(\rho E + p)) = \nabla \cdot (k_{eff} \nabla T) + S_h$$

$$\text{Where, } k_{eff} = \sum_{i=1}^{i=n} x_i k_i = x k_g + (1 - x) k_f \quad \& \quad E = \frac{\sum_{i=1}^{i=n} x_i \rho_i E_i}{\sum_{i=1}^{i=n} x_i \rho_i}$$

**Conservation of Volume Fraction**

$$\sum_{i=1}^{i=n} x_i = 1$$

$$\left(\frac{\partial}{\partial t}(x_v \rho_v) + \nabla \cdot (x_v \rho_v U)\right) = \sum_{x=1}^{x=n} \Gamma_{fv}$$

Also

$$\rho_{tp} = \sum_{i=1}^{i=n} x_i \rho_i = x \rho_g + (1 - x) \rho_f$$

$$\mu_{tp} = \sum_{i=1}^{i=n} x_i \mu_i = x \mu_g + (1 - x) \mu_f$$

$$k_{eff} = \sum_{i=1}^{i=n} x_i k_i = x k_g + (1 - x) k_f$$

The capillary tube wall specified as frictional adiabatic wall, and the content of the capillary tube as refrigerant. The boundary conditions specified for this case are as given in Table (2).

The data used in the validation are presented via table 3

## RESULTS AND DISCUSSION

### Experimental Results

First of all it is worthy to mention that **REFPROP** software is used for calculation of saturated pressure to locate the beginning of metastable region. This is done by enter the temperature along capillary tube measured experimentally into **REFPROP** for refrigerant R22 to calculate saturation pressure and plot it with measured pressure in the same chart to locate the intersection point.

**Figure (5)** displays the measured pressure and calculated saturated pressure distribution along straight adiabatic capillary tube with internal diameter of 1.4 mm, length of 100 cm. At the first 27 cm there is subcooled single phase region where the pressure drop linearly while the calculated saturated pressure remain constant due to adiabatic conditions along the wall of the capillary tube. Point (a) which is the intersection between measured pressure and calculated saturated pressure represents the beginning of metastable region. It can be seen in the region from point (a) to (b), the measured pressure still drop linearly and become less than the calculated saturated pressure while the latter remain constant. At point (c) around 70 cm from inlet, both pressures drop non-linearly due to formation of bubbles which required a latent heat of vaporization take it from liquid which lead to make a drop in calculated saturated pressure. Point (c) represents the ending of metastable region. Post point (c) there will be two phase thermodynamics equilibrium region till the end of the capillary tube. Point (c) was located from the sudden drop in calculated

saturated pressure. Mass flow rate effect on metastable region studied experimentally and the main conclusion is that as the mass flow rate increase, the intersection point of measured pressure and calculated saturated pressure will be retarded which delay the occurrence of the beginning of inception of vapor as shown **Figure (6)**. It can be seen that for straight capillary tube of length 100 cm, when the mass flow rate increases from  $M_2 = 62$  kg/hr to  $M_3 = 79$  kg/hr, the intersection point of measured pressure and calculated saturated pressure will be delayed which retard the flashing inception point and delayed the occurrence of vaporization. Also the increasing of mass flow rate will reduce the calculated saturated pressure gradient because the faster gradient mean the faster vaporization. **Figure 7** illustrates the beginning of metastable region for different mass flow rate of straight capillary tube with length 150 cm. The metastable region analysis through adiabatic helical capillary tube is presented on **Figure 8**. Table 4 displays the beginning of metastable region for straight and helical capillary tube. As the mass flow rate increases, intersection point moves downstream far from capillary tube inlet. **Figure 9** and **10** illustrates the effect of mass flow rate on metastable region of refrigerant flow through non-adiabatic helical capillary tube with internal diameter of 1.4 mm and 200 cm length with 8 cm coil diameter. In **Figure 9**, the measured pressure does not intersect the calculated saturated pressure with  $M_1 = 32$  kg/hr. The metastable flow did not appear due to conduction heat transfer between the hot capillary tube and the cold suction line makes the condensation stronger than flashing. Increasing the mass flow rate up to  $M_2 = 38$  kg/hr will make the flashing into vapor stronger than condensation which lead to metastable flow to appear. It can be seen as the mass flow rate increasing the intersection point will delay and the temperature gradient due to conduction heat transfer will be small. **Figure 11** shows the pressure distribution under adiabatic conditions for the same discharge pressure of refrigerant flow through different capillary tubes. The straight capillary tube of length 70 cm has the lowest pressure drop compared to others. The measured pressure is 1042 kPa at 7 cm length and it is 505 kPa at 63 cm length. While for straight capillary tube of length 100 cm, the pressure at 10 cm is 1034 kPa and at 90 cm the pressure is 375 kPa which mean that straight capillary tube of total length 100 cm has higher pressure drop than straight capillary tube of total length 70 cm. Also the straight capillary tube of length 100 cm has lower pressure drop compared with pressure drop through helical capillary tube with the same length and diameter under adiabatic conditions. The mass flow rate variation with discharge pressure is linear as shown in **Figure 12**. It is noticed that as the discharge pressure increased, the mass flow rate will increased too. Three different lengths of capillaries are selected 70, 100 and 150 cm, and two different helical capillary tube are selected with coiling diameter of 2 and 6 cm. The relation is linear for different straight and helical capillaries but it is less for 150 cm length. It can be seen the mass flow rate will decrease as the coiling diameter decreases. Four different lengths of adiabatic straight capillary tubes used to study the variation of mass flow rate with the length. **Figure 13** shows the relation of mass flow rate of refrigerant R22 with the length of capillary tubes. It can be seen that as the length of capillary increases, mass flow rate will decreases under the same discharge pressure. The exponential formula represents the relation of refrigerant mass flow rate with the length of capillary tube. It can be seen in **Figure 14** that as the capillary tube length increases, the mass flow rate will decreases but when the length of capillary tube increases from 100 cm to 150 cm, mass flow rate will decreases from 50 kg/hr to 42 kg/hr for the same discharge pressure of 1300 kPa. **Figures (15) to (19)** represent the pressure distribution along capillary tube under different condensation temperature. It can be seen that as the condensation temperature increases, capillary tube inlet pressure increases.

### Numerical CFD Results

The refrigerant flow characteristic through adiabatic straight capillary tube has been studied using ANSYS CFX 16.1 based on finite volume method. **Figure 20** illustrates pressure distribution modeled depending up on coarse and fine mesh which shows mesh independence so that coarse mesh has been used for all numerical results in this paper to reduce the time of iteration. The number of nodes in the case of coarse mesh is 34816 while nodes number equal to 241097 for the case of fine mesh. **Figure 21** illustrates the distribution of pressure along the length of straight capillary tube under adiabatic conditions. It can say that pressure drop is linear in the single phase region until the flashing inception point where pressure drop suddenly and non-linearly. **Figure 22** displays the temperature distribution along the capillary tube. it can be noted that it remain constant in the single phase region while it drops suddenly due to formation of vapor bubbles which require latent heat of vaporization taken from liquid which led to that decreasing of temperature. **Figure 23** demonstrates the dryness fraction along capillary tube which equals to zero in the single phase region but with the inception of vapor it starts to increasing which mean the occurrence of phase change phenomenon. **Figure 24** shows the velocity distribution along the centerline of the pipe it can be seen that it increasing with the beginning of vapor inception point and this satisfy the conservation of energy principle because the decreasing in the thermal energy converted into kinetic energy.

**Figure 25** shows a comparison between CFX model of the distribution of pressure along the capillary tube with measured data of Li et.al and with numerical data of Ingle et.al using ANSYS FLUENT 15. Again a good agreement is obtained. **Figure 26** shows a comparison of the distribution of pressure along the capillary tube predicted by present CFD model [CFX] with measured data of Li et.al and with numerical data of Zareh et.al using drift flux model. A good agreement is obtained **Figure 27** shows the comparison of present experimental and numerical investigation of three different lengths. A fairly good agreement is obtained. **Figure 28** displays another comparison between experimental and numerical results. **Figure 29** displays the comparison between present experimental results with experimental data **Chen and Lin** of refrigerant flow through non-adiabatic straight capillary tube. It can be seen that obtained measured data is within acceptable accuracy.

### CONCLUSIONS

- Parametric study was presented including the effect of length of capillary tube, coiling diameter and mass flow rate on the beginning of metastable region
- The length of capillary tube has a strong effect where it was found that as length of capillary tube increases, flashing inception point is retarded which lead to increase single phase length and delay the occurrence of vaporization.
- The coiling diameter has a strong effect too on beginning of metastable region where it is obtained that it delay the beginning of metastable region under the same length of capillary tube.
- The mass flow rate is an influence parameter on beginning of metastable region where as mass flow rate increases, vaporization will be delayed.
- For the non-adiabatic helical capillary tube, the mass flow rate is the most influence parameter on beginning of metastable region. It was found that as mass flow rate increases, the conduction heat transfer between capillary tube and suction line will be weak and metastable region will appear.

- Mass flow rate of refrigerant flow through straight capillary tube is higher than that through helical capillary tube due to secondary flow effect of coiling which produces centrifugal force in addition to frictional force lead to resist the flow.

**Table.1:** Measured mass flow rate for each capillary tube type

Capillary tube	M1[kg/hr]	M2[kg/hr]	M3[kg/hr]	M4[kg/hr]	M5[kg/hr]
Straight, L = 150 cm	42	54	68	87	98
Straight, L = 100 cm	50	62	79	92	100
Straight, L = 70 cm	60	70	85	100	111
Straight, L = 50 cm	65	78	91	101	119
Helical, D = 6 cm	48	60	75	82	95
Helical, D = 2 cm	44	59	66	77	88
Straight , L = 150 cm	34	44	55	60	67
Helical, D = 8 cm	32	38	61	65	71

**Table 2:** Boundary conditions

Zone	Parameter
Upstream Conditions	<ul style="list-style-type: none"> <li>• Inlet Pressure</li> <li>• Inlet Temperature</li> <li>• Inlet Dryness Fraction Specified 1 for Sub-Cooled Liquid</li> </ul>
Downstream Conditions	<ul style="list-style-type: none"> <li>• Exit Pressure</li> </ul>
Wall	<ul style="list-style-type: none"> <li>• Adiabatic Frictional Wall</li> </ul>

**Table 3** Test Flow conditions for refrigerant

Case Study	$P_{in}$ [kPa]	$T_{in}$ [°K]	d	$e/d$
Case 1	967	304.4	1.17	$3.0303 * 10^{-3}$
Case 2	858	303	0.66	$2.991 * 10^{-3}$

**Table.4:** Flashing inception point location corresponding to the mass flow rate

M[kg/hr]	X1[cm]	X2[cm]	X3[cm]
M1		39	15
M2	10	43	22
M3	20	45	32
M4	23	45	32
M5	27	-	-

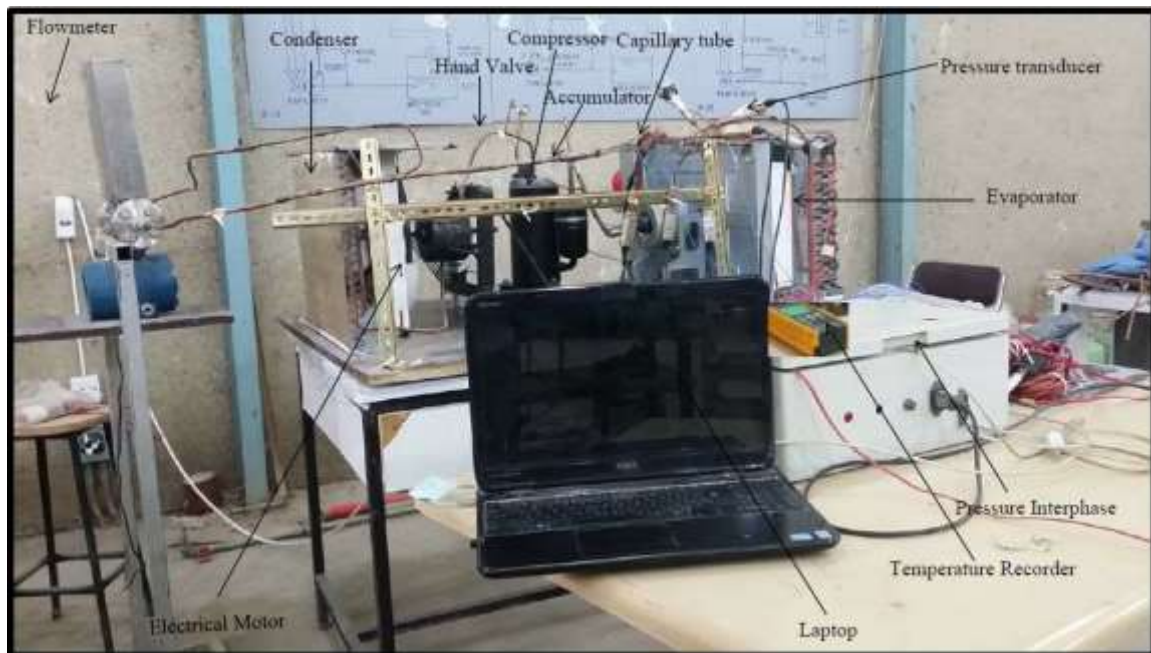


**Figure (1a):** Plate of experimental apparatus

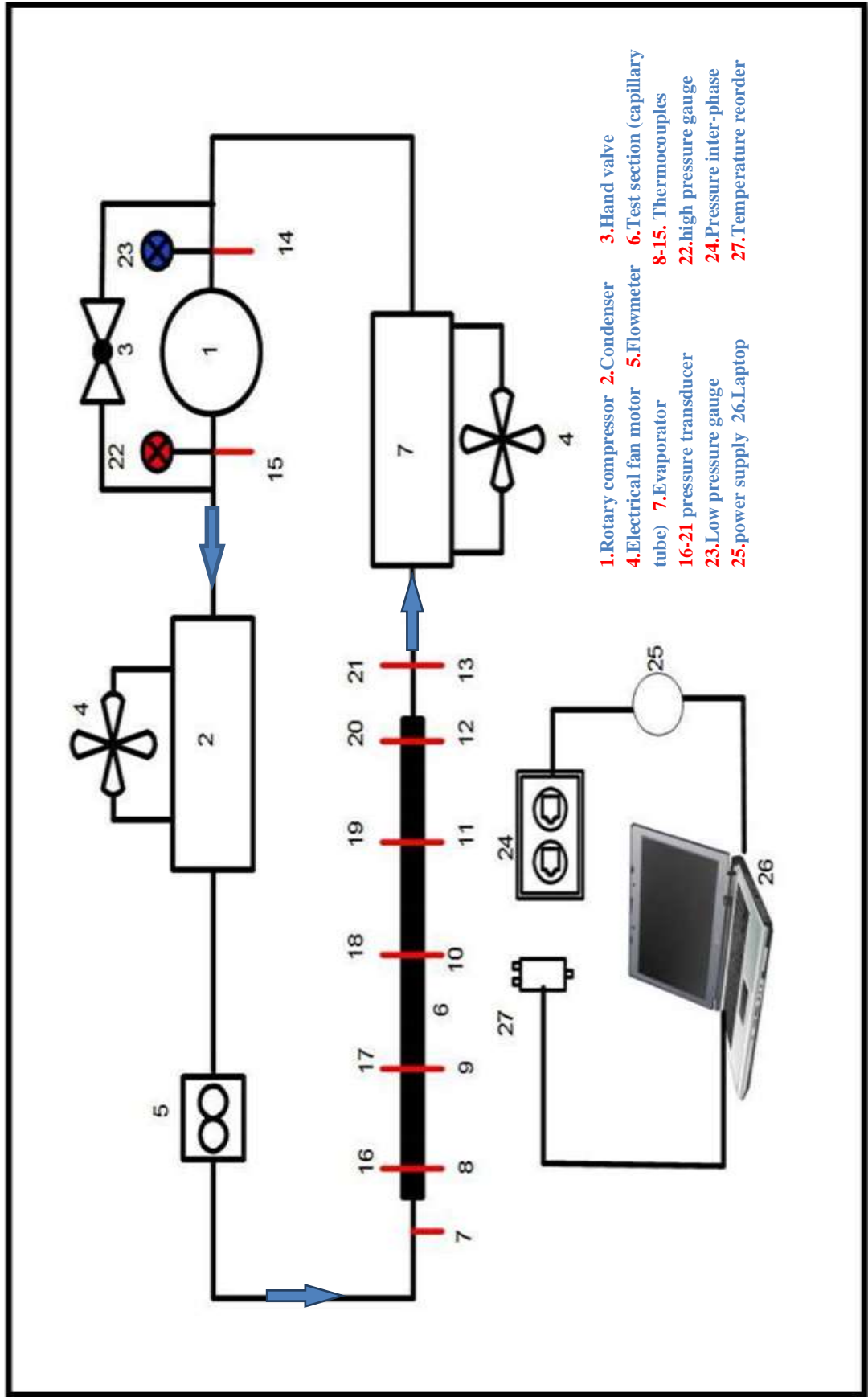


Figure (1b) : Schematic representation of experimental apparatus



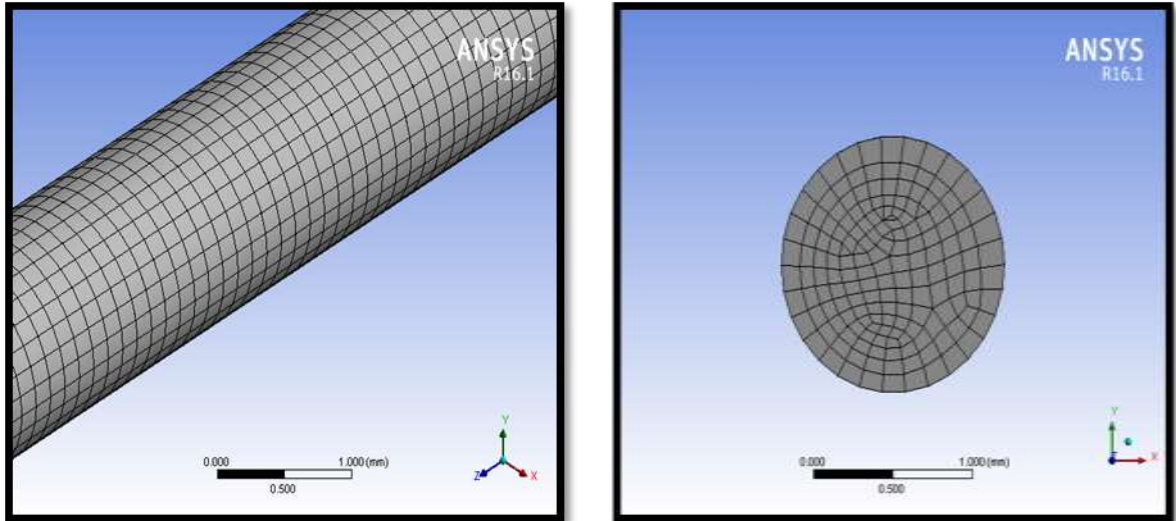
Figure (2): T-connection of pressure sensor to the capillary tube

	Straight			Helical	
Shape of capillary tube					
Length (cm)	150	100	70	100	100
diameter (mm)	1.4	1.4	1.4	1.4	1.4
Coil diameter (cm)	—	—	—	2	6

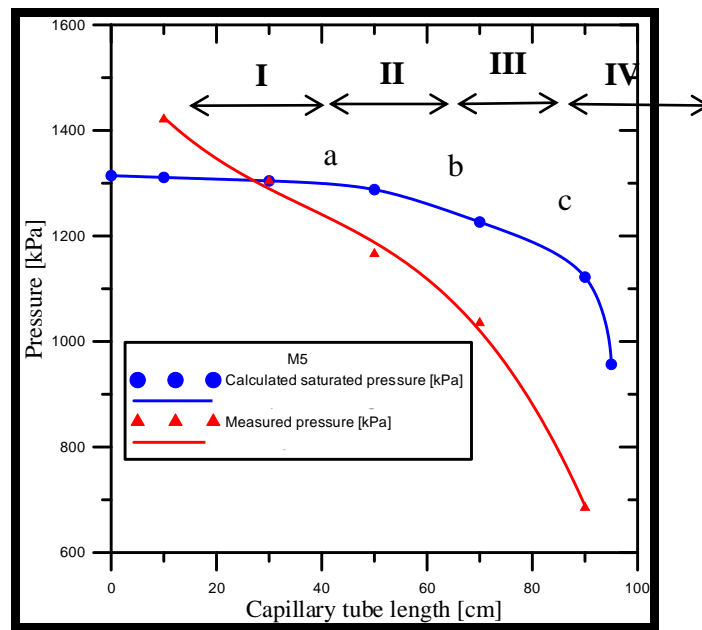
  

	Straight	Helical
Shape of capillary tube		
Length (cm)	150	200
diameter (mm)	1.4	1.4
Coil diameter (cm)	—	8

Figure (3): Adiabatic and Non-adiabatic straight and helical capillary tubes



**Figure (4):** Mesh of capillary tube



**Figure (5):** The measured pressure with calculated saturated pressure of refrigerant R22 flow through adiabatic straight capillary tube

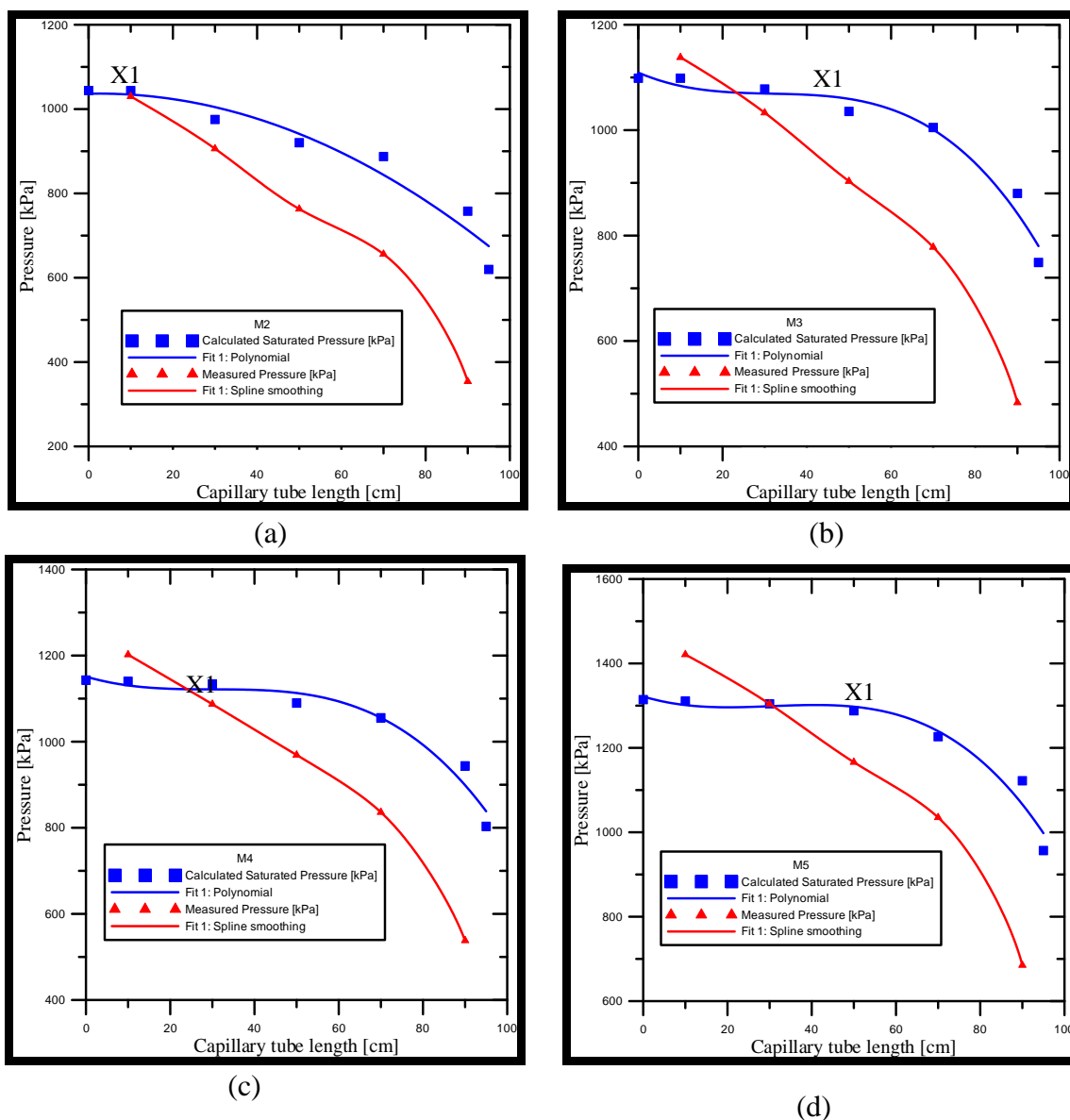


**Figure (6):** Measured pressure and calculated saturated pressure of refrigerant flow through adiabatic straight capillary tube under different mass flow rate,  $L = 100$  cm

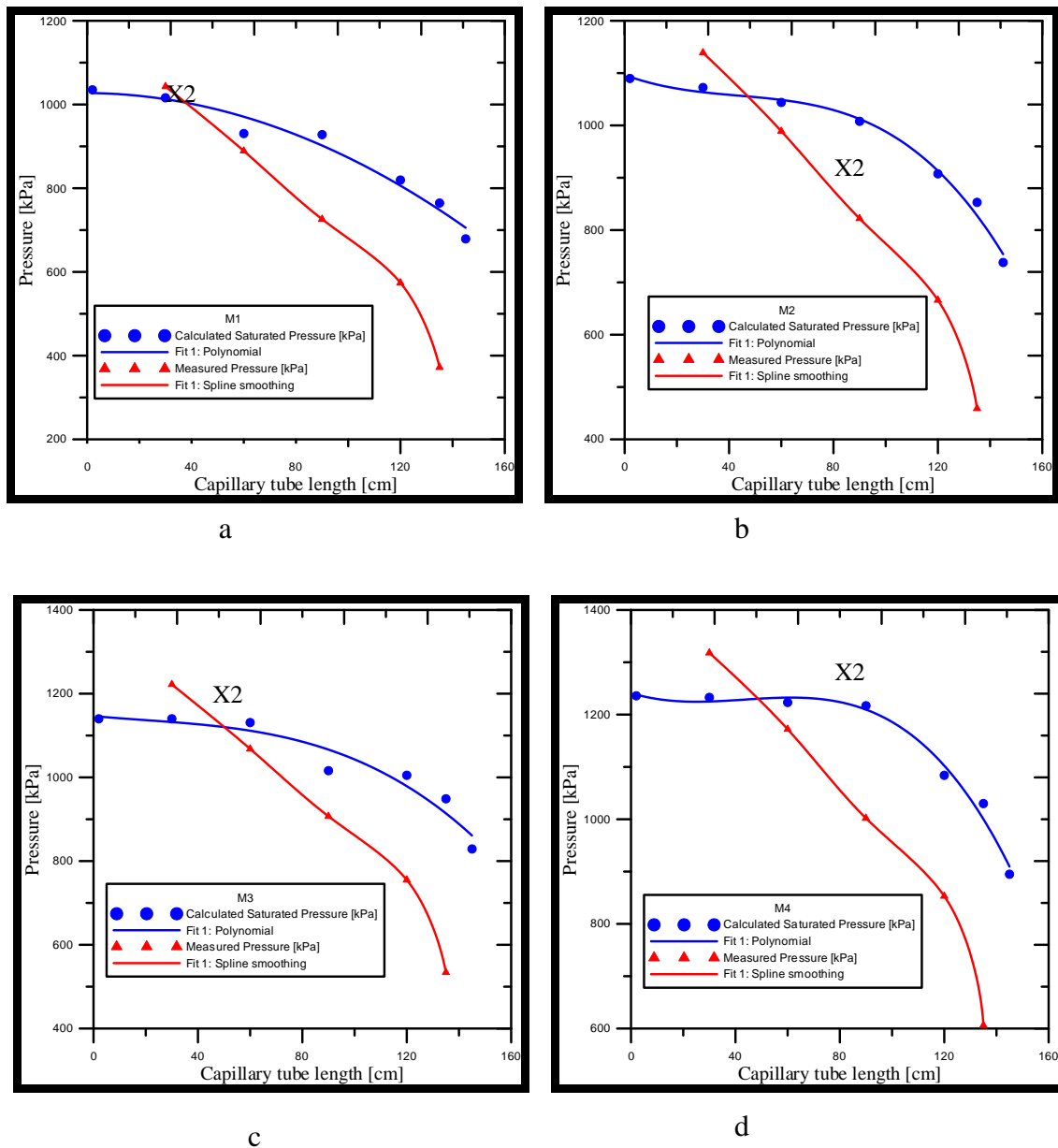


**Figure (7) :** Measured pressure and calculated saturated pressure of refrigerant flow through adiabatic straight capillary tube under different mass flow rate,  $L = 150$  cm

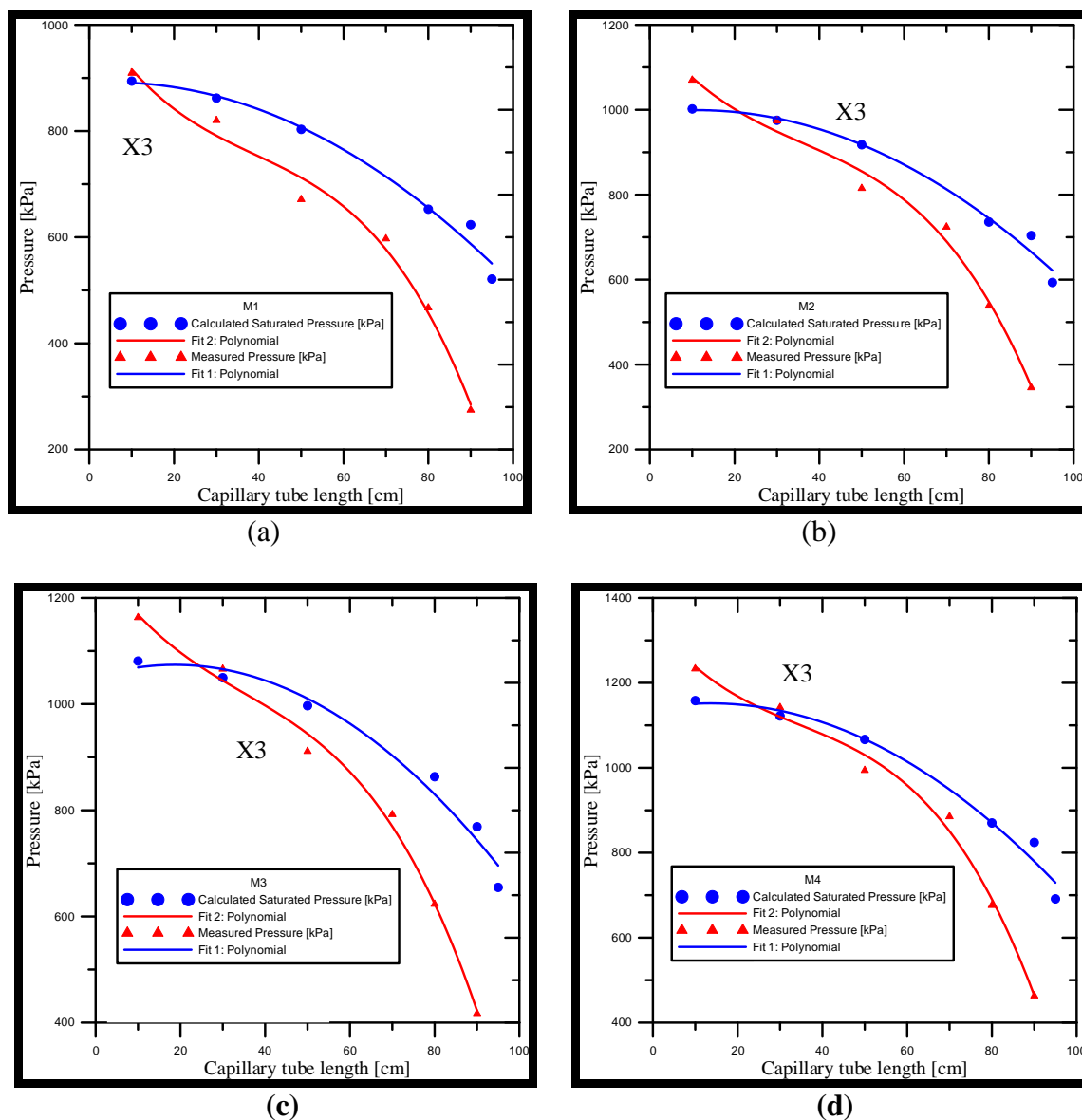


**Figure (8):** Effect of mass flow rate of refrigerant R22 flow through adiabatic helical capillary tubes of coil diameter 6 cm on flashing inception point,  $L = 100$  cm

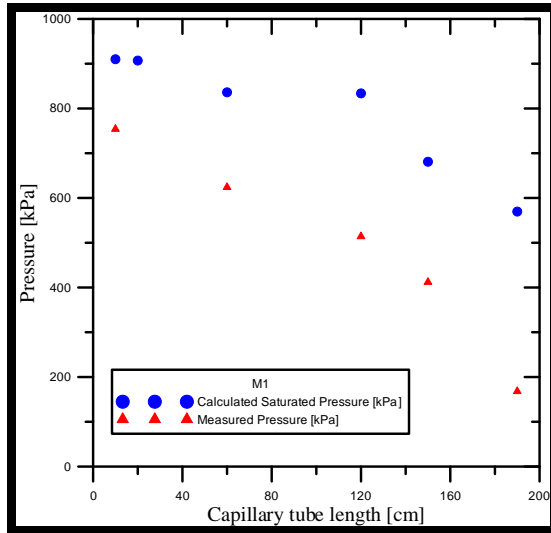


**Figure (9):** Distribution of measured pressure and calculated saturated pressure along non-adiabatic helical capillary tube without metastable region

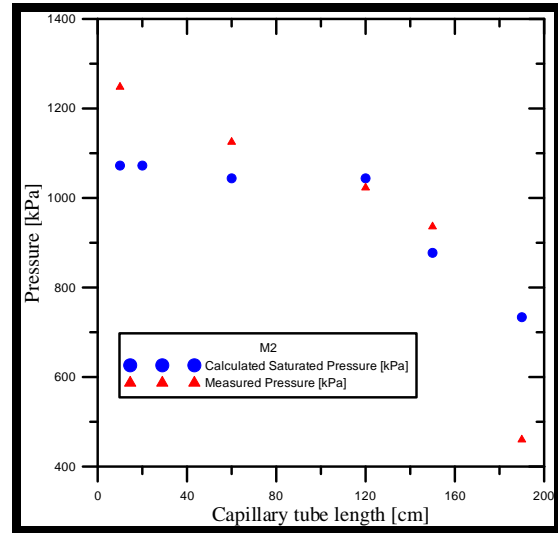


**Figure (10):** Distribution of measured pressure and calculated saturated pressure along non-adiabatic helical capillary tube metastable region appear

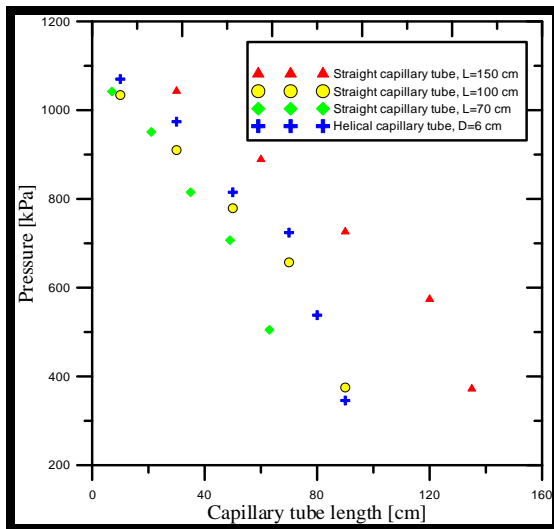


**Figure (11):** Distribution of measured pressure along different types of capillaries

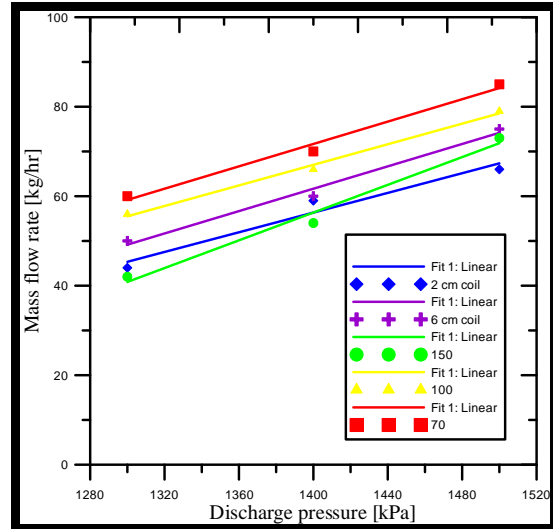


**Figure (12):** Variation of refrigerant mass flow rate with discharge pressure

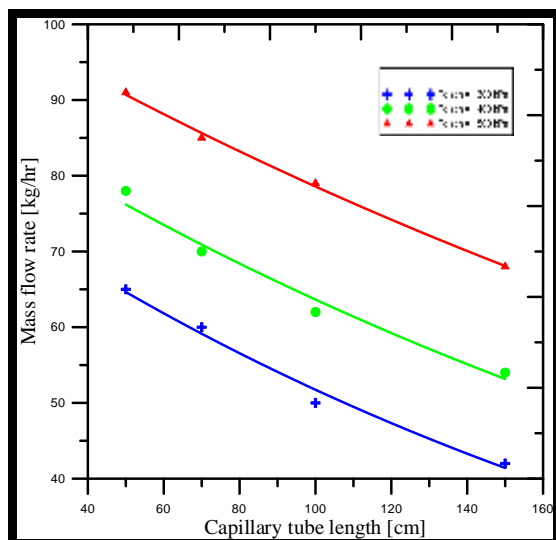


**Figure (13):** Relation of mass flow rate with capillary tube length

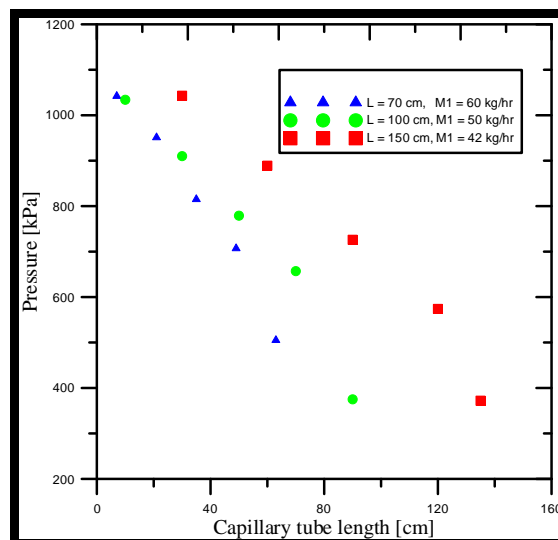


**Figure (14):** Pressure variation along straight adiabatic capillary tube length for different length under the same condensing pressure

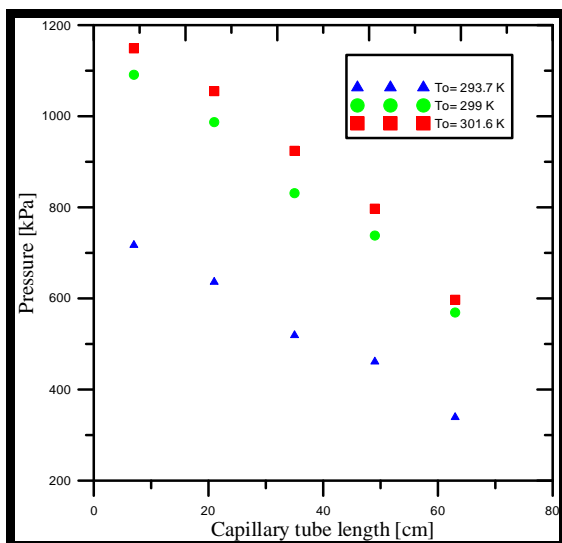


**Figure (15):** Pressure distribution of refrigerant along adiabatic straight capillary tube,  $L=70$  cm

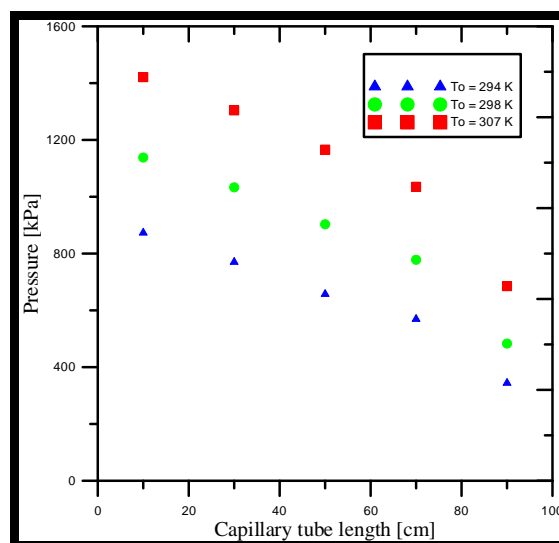


**Figure (16):** Pressure distribution of refrigerant along adiabatic straight capillary tube,  $L=100$  cm

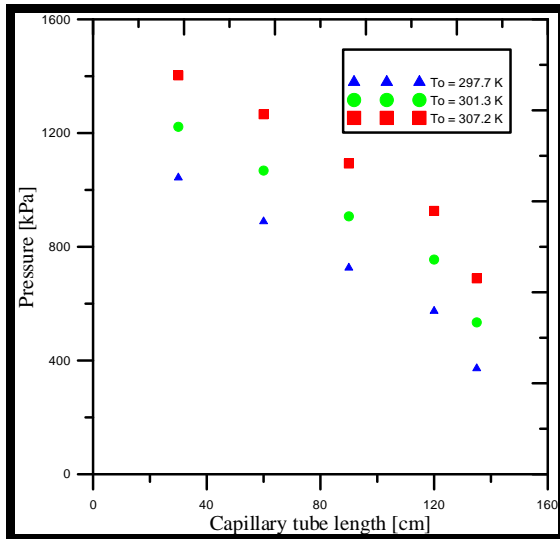


**Figure (17):** Pressure distribution of refrigerant along adiabatic straight capillary tube, L=150cm

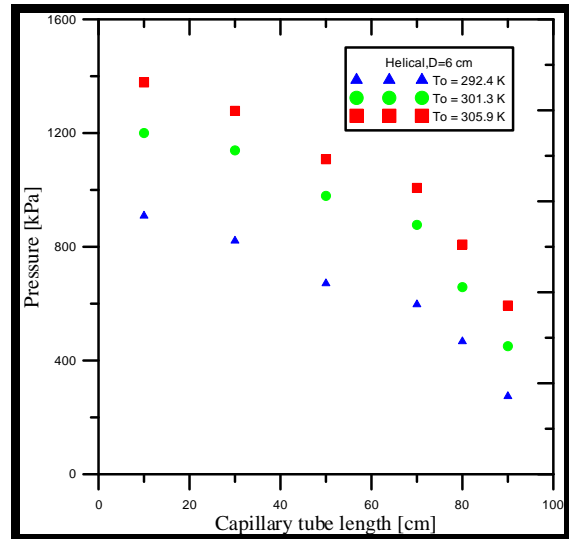


**Figure (18):** Pressure distribution of refrigerant along adiabatic helical capillary tube, L=100cm, D=6 cm

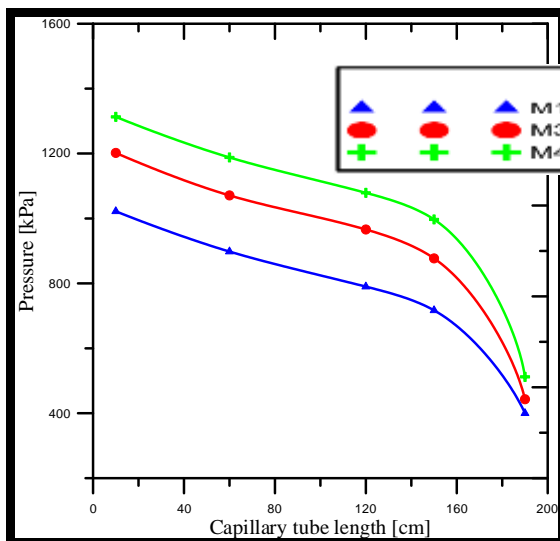


**Figure (19):** Pressure distribution of refrigerant along non-adiabatic helical capillary tube, L=200cm, D=8 cm

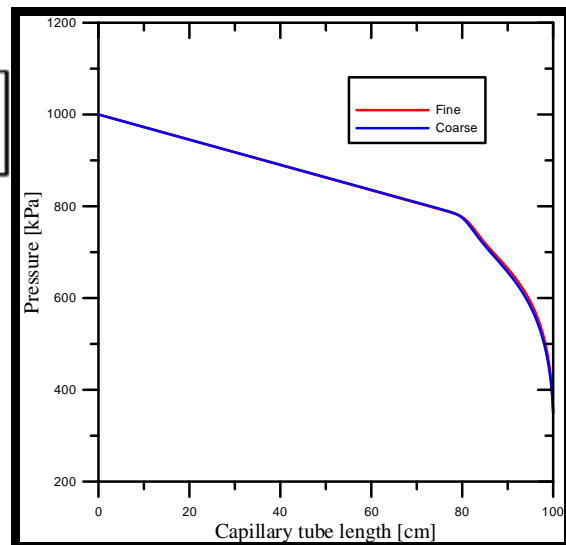


**Figure (20):** Pressure distribution for different mesh sizes

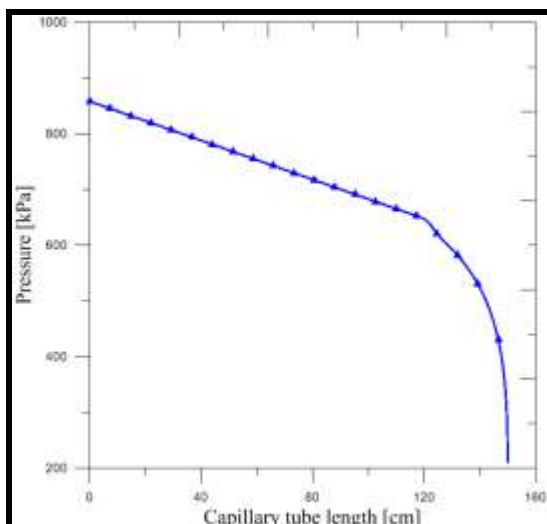


Figure (21): pressure distribution along capillary tube

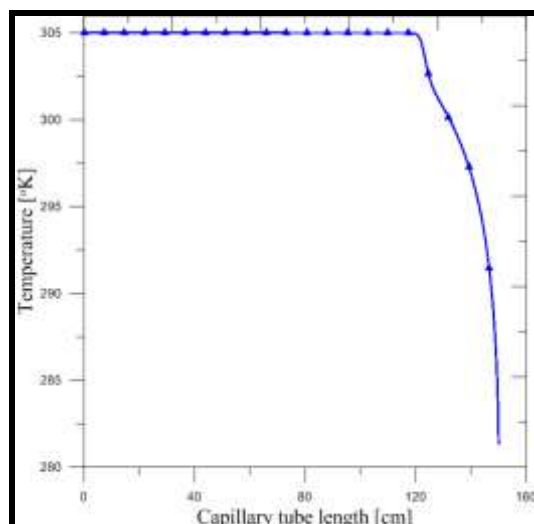


Figure (22): Temperature distribution along capillary tube

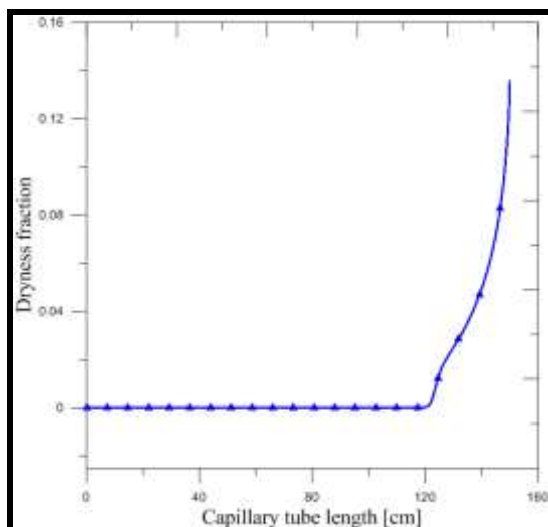


Figure (23): Dryness fraction distribution along capillary tube

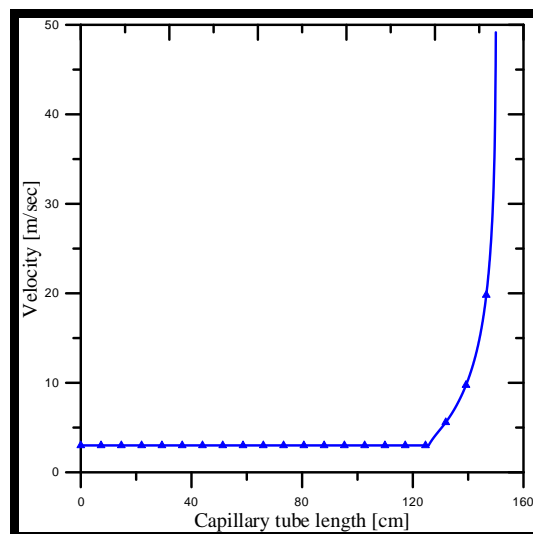
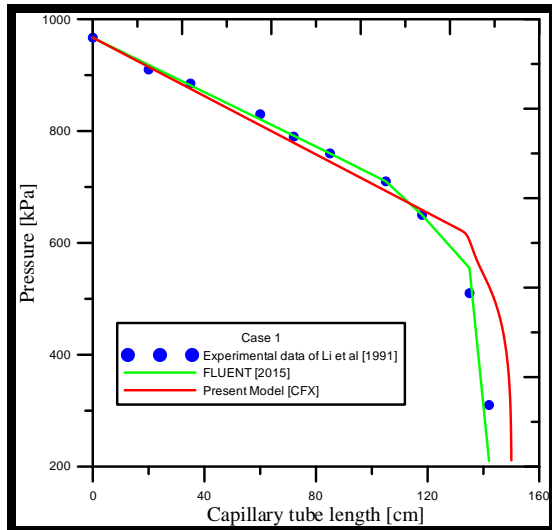
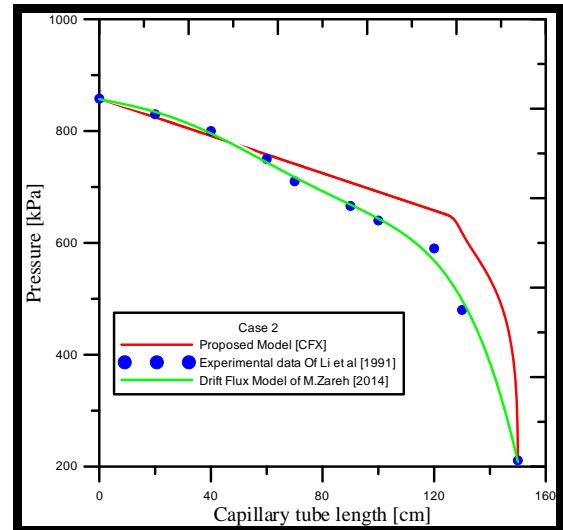


Figure (24): Velocity distribution along capillary tube



**Figure (25):** A Comparison of present numerical model with Ingle et.al and experimental data points of Li et al



**Figure (26):** A Comparison of present numerical model with M.Zareh model and experimental data points of Li et al

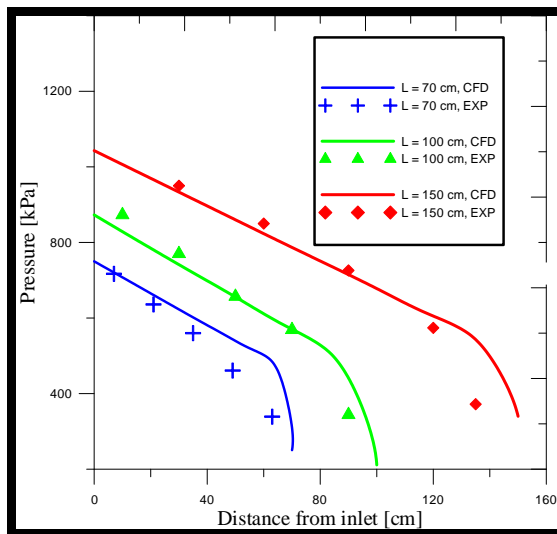


**Figure (27):** A Comparison Pressure distribution of refrigerant flow inside straight capillary tube under adiabatic conditions for different lengths

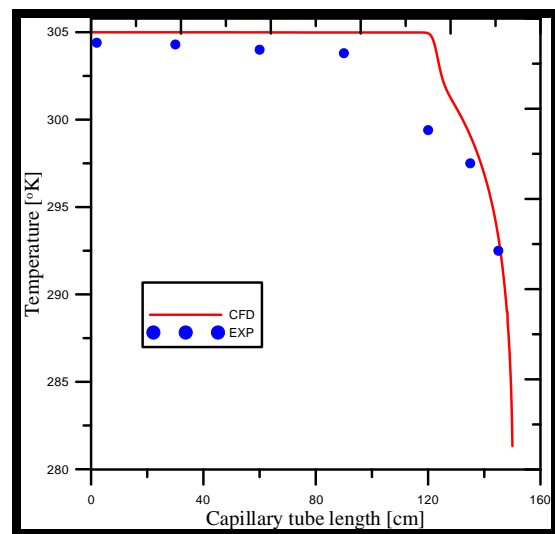


**Figure (28):** A Comparison of temperature distribution between present experimental work with present numerical model [CFX] of refrigerant flow through adiabatic straight capillary tube

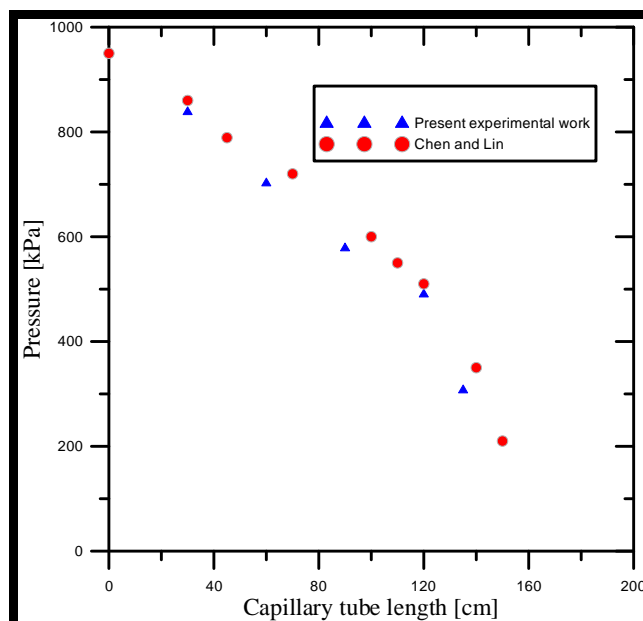


**Figure (29):** A Comparison of pressure distribution of present experimental work with Chen and Lin (2001) for refrigerant flow through non-adiabatic straight capillary tube

## REFERENCES

ANSYS CFX 16.1 Documentation, 2015

Bansal, P., & Rupasinghe, A. (1998). An homogeneous model for adiabatic capillary tubes. *applied thermal engineering*, 18(3), pp. 207-219.

Chen, D. and Lin, S., (2001). Underpressure of vaporization of refrigerant R-134a through a diabatic capillary tube. *International Journal of refrigeration*, 24(3), pp.261-271.

Huerta, A. A. S., Fiorelli, F. A. S., & de Mattos Silveiras, O. (2007). Metastable flow in capillary tubes: An experimental evaluation. *Experimental thermal and fluid science*, 31(8), pp. 957-966 .

Ingle, R., Rao, V. S., Mohan, L .S., Dai, Y., Inc, A., & Chaudhry, G. (2015). Modelling of Flashing in Capillary Tubes using Homogeneous Equilibrium Approach. *Procedia IUTAM*, 15, pp. 286-292 .

Imran , A. A. "Adiabatic and Separated Flow of R-22 and R-407C in Capillary Tube" *Eng. & Tech. Journal* ,Vol. 27, No. 6, 2009

Li, R.-Y., Lin S., Chen, Z.-Y., & Chen, Z.-H. (1990). Metastable flow of R12 through capillary tubes. *International Journal of Refrigeration*, 13(3), pp. 181-186 .

Liang, S., & Wong, T. (2001). Numerical modeling of two-phase refrigerant flow through adiabatic capillary tubes. *applied thermal engineering*, 21(10), pp. 1035-1048 .

NIST, Thermodynamics and transport properties of refrigerants and refrigerants mixtures-REFPROP

Prajapati, Y. K., Pathak, M., & M. K. Khan (2016). Computational Fluid Dynamics Modeling of Two- Phase Flow in an Adiabatic Capillary Tube. *Journal of Thermal Science and Engineering Applications*, 7(1), 011006.

Zareh, M., Shokouhmand, H., Salimpour, M. R., & Taeibi, M. (2014). Numerical simulation and experimental analysis of refrigerants flow through adiabatic helical capillary tube. *International Journal of Refrigeration*, 38, pp. 299-309.